

Three-dimensional model of cytochrome P450 human aromatase

CEDRIC LOGE¹, MARC LE BORGNE¹, PASCAL MARCHAND¹, JEAN-MICHEL ROBERT¹,
GUILLAUME LE BAUT¹, MARTINA PALZER², & ROLF W. HARTMANN²

¹Département de Pharmacochimie, Biomolécules et Cibles Thérapeutiques, UPRES EA1155, UFR Sciences Pharmaceutiques, 1 rue Gaston Veil, F-44035 Nantes cedex 1, France, and ²Pharmazeutische und Medizinische Chemie, Universität des Saarlandes, P.O. Box 151150, D-660041 Saarbrücken, Deutschland

(Received 5 January 2005; accepted 3 March 2005)

Abstract

A three-dimensional (3-D) structure of human aromatase (CYP19) was modeled on the basis of the crystal structure of rabbit CYP2C5, the first solved X-ray structure of an eukaryotic cytochrome P450 and was evaluated by docking *S*-fadrozole and the steroidal competitive inhibitor (19*R*)-10-thiiranylestr-4-ene-3,17-dione, into the enzyme active site. According to a previous pharmacophoric hypothesis described in the literature, the cyano group of *S*-fadrozole partially mimics the steroid backbone C(17) carbonyl group of (19*R*)-10-thiiranylestr-4-ene-3,17-dione, and was oriented in a favorable position for H-bonding with the newly identified positively charged residues Lys119 and Arg435. In addition, this model is consistent with the recent combined mutagenesis/modeling studies already published concerning the roles of Asp309 and His480 in the aromatization of the steroid A ring.

Keywords: Breast cancer, CYP19, aromatase, homology modeling, active site, inhibitors, *S*-fadrozole

Introduction

Breast cancer is the most frequent cancer amongst women. Laboratory work in this therapeutic field aims at developing structures able to inhibit human cytochrome P450 aromatase, also called CYP19. This enzyme is a member of the heme-containing cytochrome P450 superfamily which requires 3 moles of oxygen and 3 moles of NADPH to function for every mole of C(19) steroid metabolized [1,2]. CYP19 catalyses the bioconversions of androgens (androstenedione, testosterone) into estrogens (estrone, estradiol), through the aromatization of the A ring (Figure 1). In this process, the 19-methyl is removed. Taking into account the known proliferative effects of estrogens, CYP19 constitutes an important target in the treatment strategy of hormone-dependent breast cancers in postmenopausal women. Aromatase

inhibitors may be divided into two major classes, the steroidal and the non-steroidal compounds (Figure 2). The steroidal compounds such as formestane and exemestane—also referred to as type I agents or inactivators—are analogues of androstenedione and bind competitively but irreversibly to the substrate-binding site of the enzyme [3,4]. The non-steroidal inhibitors, previously termed type II inhibitors, interfere competitively but reversibly with the heme Fe²⁺ ion of the cytochrome P450 moiety of aromatase. Marketed non-steroidal inhibitors include the prototype aminoglutethimide (first-generation) andazole derivatives such as fadrozole (second-generation), letrozole and anastrozole (third-generation) [5,6]. Recent efforts are being carried out both to identify new molecules of therapeutic interest and to clarify the mechanism of action that could be improved by a better knowledge of the enzyme's active site. However,

Correspondence: C. Loge, Département de Pharmacochimie, Biomolécules et Cibles Thérapeutiques, UPRES EA1155, UFR Sciences Pharmaceutiques, 1 rue Gaston Veil, F-44035 Nantes cedex 1, France. Tel: 33 240 411 108. Fax: 22 240 412 876. E-mail: cedric.loge@univ-nantes.fr

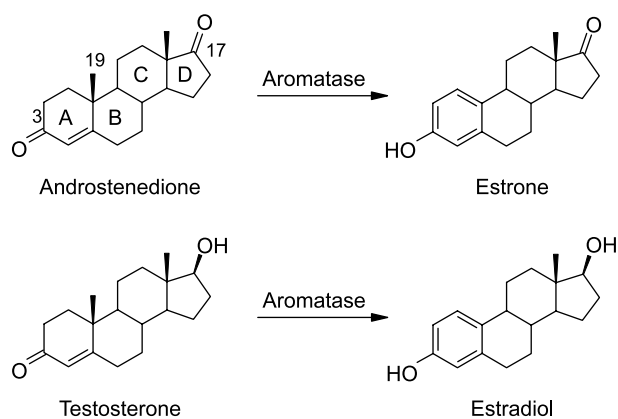


Figure 1. Aromatization of androstenedione and testosterone to estrone and estradiol, respectively.

crystallization of the human membrane-bound enzyme has been difficult to accomplish, and only this result would allow an X-ray analysis of the structure. So far, numerous molecular models of aromatase have been published [7–12], but all are based on the crystallographic data of P450cam (CYP101), terp (CYP108) and bm3 (CYP102), coming from bacterial sources whose percent sequence identity with aromatase ranges from 13–18%. In 2000, the crystal structure of rabbit CYP2C5 was reported as the first solved X-ray structure of a

mammalian microsomal cytochrome P450 [13]. This prompted us to construct a 3-D structure of human CYP19, by the homology modeling technique, using the structure of CYP2C5 complexed with a relatively general inhibitor of human 2C enzymes as a template [14].

Materials and methods

Molecular modeling studies were performed using Sybyl software version 6.9.1[†] running on a Silicon Graphics Octane workstation. The crystallographic structure of rabbit P450 2C5 complexed with a substrate, 4-methyl-*N*-methyl-*N*-(2-phenyl-2*H*-pyrazol-3-yl)benzene sulfonamide (DMZ), at 2.3 Å resolution (pdb code: 1N6B) was used as a template [14]. The amino acid sequence of the human aromatase was aligned to that of the rabbit P450 2C5 using ClustalW [15]. This alignment was further checked by comparing a secondary structure elements prediction for aromatase, obtained through the PSIPRED protein structure prediction server [16], with the experimental secondary structure assignments for CYP2C5 deduced from the PDB file. The 3-D model of the human aromatase was then constructed by the Nest program from the protein structure modeling package JACKAL [17]. The resulting model was subjected to an energy minimization using Powell's method

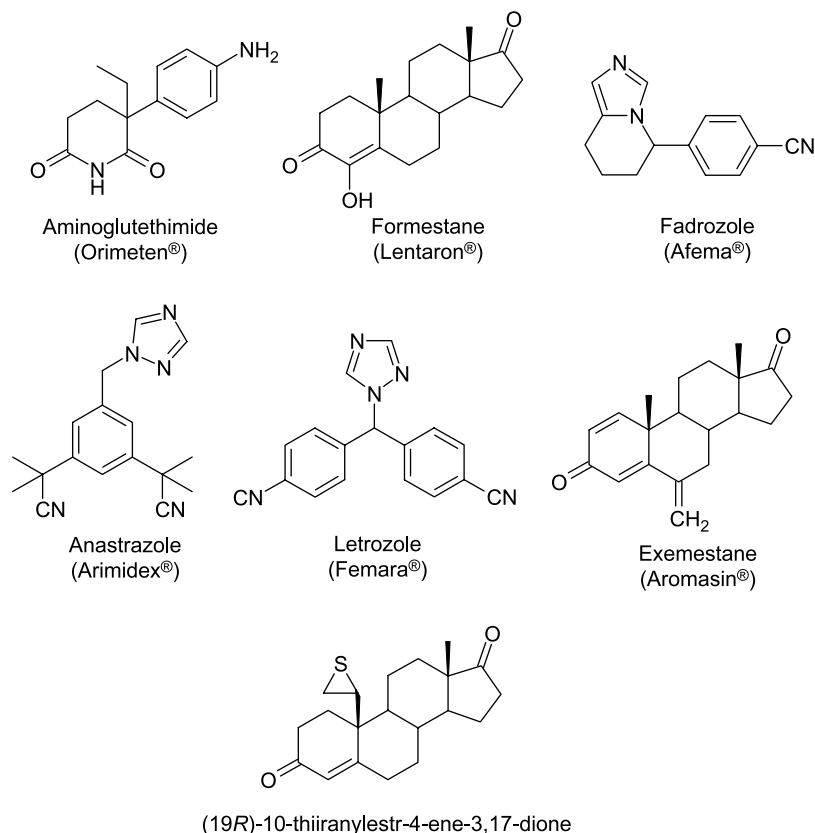


Figure 2. Chemical structures of some aromatase inhibitors.

available in Maximin2 procedure with the Tripos force field [18] and a dielectric constant of 4.0 until the gradient value reached 0.1 kcal/mol Å. Energy minimization was started with the core side chains, then the core main chains. The structure was periodically checked by the Sybyl ProTable module. If present, improper geometries were manually corrected and the structure minimized again with the above procedure. Heme extracted from the rabbit P450 2C5 structure was added to the human aromatase model, and residues neighboring heme were minimized to avoid steric conflicts.

The 3-D structures of *S*-fadrozole and (19*R*)-10-thiiranylestr-4-ene-3,17-dione were constructed using the standard sketch procedure of Sybyl and their geometries were subsequently optimized using the Tripos force field including the electrostatic term calculated from Gasteiger and Hückel atomic charges. Powell's method available in Maximin2 procedure was used for energy minimization until the gradient value was smaller than 0.001 kcal/mol Å. Flexible docking of these compounds into the enzyme active site was performed using GOLD software [19]. For each compound, the most stable docking model was selected according to the best scored conformation predicted by the GoldScore scoring function. The complexes were energy-minimized using Powell's method available in Maximin2 procedure with the Tripos force field and a dielectric constant of 4.0, until the gradient value reached 0.05 kcal/mol Å.

Results and discussion

Homology modeling of aromatase

We constructed the 3-D structure of human CYP19 using the crystal structure of the rabbit CYP2C5 complexed with a dimethyl derivative of sulfaphenazole as a template [14]. As a result of the increased resolution (2.3 vs. 3.0 Å), the overall geometry of CYP2C5 is improved relative to the previously published structure [13]. Sequence alignment was performed as described in Materials and methods section, and the results are shown in Figure 3. The N-terminal residues Met1-Ile47 were not constructed because the coordinates of the corresponding region of CYP2C5 were not determined. Sequence identity between CYP2C5 and aromatase is about 20%.

Highly conserved and functionally important residues in the CYP superfamily are: (i) three absolutely conserved residues, ExxR in the K helix and C just before the L helix (for example Glu362, Arg365 and Cys437 in CYP19); (ii) the consensus sequence (A/G)xx(E/D)T in the center of the I helix around the conserved Thr residue (Thr310 in Cyp19); (iii) the consensus sequence F(G/S)xGx(R/H)xCxGxx(I/L/F)A containing the cysteine (Cys437 in CYP19) responsible for heme binding

[20]. As shown in Figure 3, these important sequences of both CYPs are correctly aligned with each other. In addition, from Figure 3, it results that the secondary structure element predictions for aromatase (*H* = helix; *E* = strand) match reasonably well with the secondary structure elements determined in CYP2C5 by X-ray analysis. This correspondence, despite the low degree of homology between the two sequences, might confer an acceptable feasibility to the aromatase model.

The heme is sandwiched between the L helix including its N-terminal loop and the I helix. The sulfide of Cys437 provides the axial ligand at the fifth coordination site of the heme iron (Figure 4). Coordination of the heme iron by a cysteine plays a central role in the capacity of P450s to catalyze the scission of dioxygen bound to the sixth coordination site of the heme iron. The structural conservation of the heme binding site is likely to reflect structural features necessary to preserve the capacity of P450s to catalyze this reaction [13]. The propionate side chains of the heme interact with Arg435 before the L helix, Trp141 and Arg145 in the C helix, three highly conserved residues across mammalian P450s, and with Lys376 in a β -strand (Figure 4).

Amino acids whose side chains face the active site pocket are the hydrophobic residues Leu122, Ile125, Phe134, Trp224, Ile229, Ala306, Ala307, Val369, Val370, Leu372, Val373, Met374, Leu477 and Leu479, and the hydrophilic residues Lys119, Asp309, Thr310, Arg375, Lys376, Arg435, Ser478 and His480 (Figure 5).

Binding site evaluation

In order to assess the validity of our model, *S*-fadrozole, responsible for the high aromatase inhibitory activity, and the steroidal competitive inhibitor (19*R*)-10-thiiranylestr-4-ene-3,17-dione (Figure 2) were docked into the active site as described in Materials and methods section, and their positions together with some surrounding residues are shown in Figure 6. Both inhibitors coordinate to the iron atom of the heme group present at the active site of the enzyme by their imidazole and thiirane rings. According to previous studies [2,21], the 4-cyano-benzyl moiety present in *S*-fadrozole partially mimics the steroid backbone C(17) carbonyl group of (19*R*)-10-thiiranylestr-4-ene-3,17-dione, assuming that the binding mode is representative of that of the natural substrate androstenedione [21,22]. In addition, as suggested by S. Chen et al. [23], the C(17) carbonyl binding region of the active site could anchor the D ring of the steroid or participate in binding various electronegative groups of inhibitors by acting as hydrogen bond donor with the positively charged residues Lys119 and Arg435.

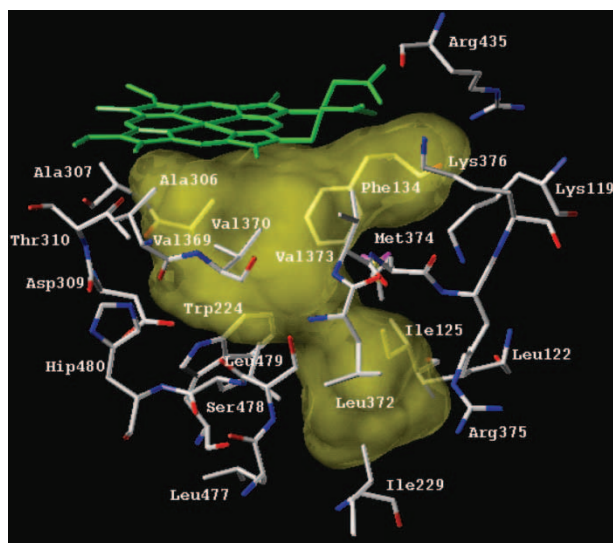


Figure 5. Heme and amino acid residues constituting the active site pocket.

Conclusion

In summary, we have developed a new model of aromatase based on the crystal structure of rabbit CYP2C5, and studied the docking of *S*-fadrozole and (19*R*)-10-thiiranylestr-4-ene-3,17-dione into the enzyme active site.

According to the pharmacophoric hypothesis described by P. Furet et al. [21], the cyano group of *S*-fadrozole partially mimics the steroid backbone C(17) carbonyl group of (19*R*)-10-thiiranylestr-4-ene-3,17-dione, and was oriented in a favorable position for H-bonding with the new identified

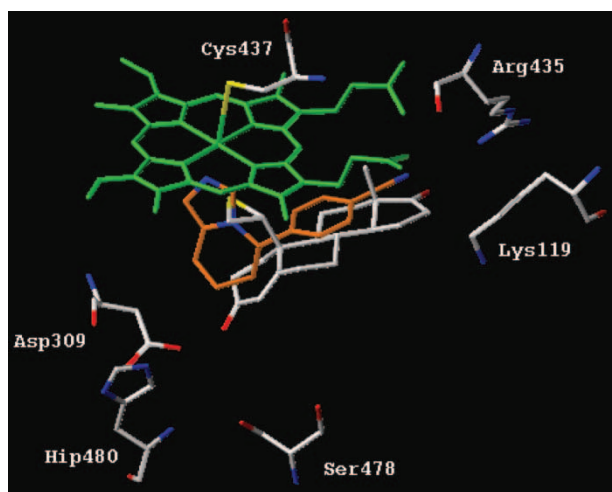


Figure 6. Best docking solutions of *S*-fadrozole and (19*R*)-10-thiiranylestr-4-ene-3,17-dione into the enzyme active site.

positively charged residues Lys119 and Arg435. In addition, our model is consistent with the recent combined mutagenesis/modeling studies published by Y. C. Kao et al. concerning the roles of Asp309 and His480 in the aromatization of the steroid A ring [24].

This new model will help us to formulate strategies for design of new aromatase inhibitors. Mutagenesis studies on the newly identified amino acids Lys119 and Arg435 should confirm or disagree with our hypotheses.

Note

[†]Sybyl 6.9.1, Tripos Associates, Inc. 1699 South Hanley Road, St. Louis, MO 63144, USA.

References

- [1] Thompson EA, Siiteri PK. *J Biol Chem* 1974;249:5373.
- [2] Ahmed S. *Drug Des Discov* 1998;15:239.
- [3] Johnston SR, Dowsett M. *Nat Rev Cancer* 2003;3:821.
- [4] Lonning PE. *Endocr Relat Cancer* 2004;11:179.
- [5] Mokbel K. *Int J Clin Oncol* 2002;7:279.
- [6] Miller WR. *Semin Oncol* 2003;30:3.
- [7] Auvray P, Nativelle C, Bureau R, Dallemagne P, Séralini GE, Sourdain P. *Eur J Biochem* 2002;269:1393.
- [8] Laughton CA, Zvelebil MJ, Neidle SJ. *Steroid Biochem Mol Biol* 1993;44:399.
- [9] Koymans LMH, Moereels H, Vanden Bossche H. *Steroid Biochem Mol Biol* 1995;53:191.
- [10] Graham-Lorence S, Amarneh B, White RE, Peterson JA, Simpson ER. *Protein Sci* 1995;4:1065.
- [11] Zhou D, Cam LL, Laughton CA, Korzekwa KR, Chen S. *J Biol Chem* 1994;269:19501.
- [12] Cavalli A, Greco G, Novellino E, Recanatini M. *Bioorg Med Chem* 2000;8:2771.
- [13] Williams PA, Cosme V, Sridhar EF, Johnson DE, McRee DE. *J Inorg Biochem* 2000;81:183.
- [14] Wester MR, Johnson EF, Marques-Soares C, Dansette PM, Mansuy D, Stout CD. *Biochemistry* 2003;42:6370.
- [15] Thompson JD, Higgins DG, Gibson TJ. *Nucleic Acids Res* 1994;22:4673.
- [16] McGuffin LJ, Bryson K, Jones DT. *Bioinformatics* 2000;16:404, <http://bioinf.cs.ucl.ac.uk/psipred/>.
- [17] Xiang Z, Honig B. *J Mol Biol* 2001;421, <http://trantor.bioc.columbia.edu/programs/jackal/>.
- [18] Clarck M, Cramer III, RD, Van Opdenbosch N. *J Comput Chem* 1989;10:982.
- [19] Jones G, Willett P, Glen RC. *J Mol Biol* 1995;245:43.
- [20] Graham-Lorence S, Peterson JA. *Methods Enzymol* 1996;272:315.
- [21] Furet P, Batzl C, Bhatnagar A, Francotte E, Rihs G, Lang M. *J Med Chem* 1993;36:1393.
- [22] Kellis TJ, Childers WE, Robinson CH, Vickery LE. *J Biol Chem* 1987;262:4421.
- [23] Chen S, Zhang F, Sherman MA, Kijima I, Cho M, Yuan YC, Toma Y, Osawa Y, Zhou D, Eng ET. *J Steroid Biochem Mol Biol* 2003;86:231.
- [24] Kao YC, Korzekwa KR, Laughton CA, Chen S. *Eur J Biochem* 2001;268:243.